Pergamon

J. Geodynamics Vol. 26, No. 2–4, pp. 217–231, 1998

PII: S0264-3707(97)00050-1
0264-3707/98 $19.00+0.00

A MODEL FOR THE 1995 KOZANI–GREVENA SEISMIC SEQUENCE

B. C. PAPAZACHOS,[1]* B. G. KARAKOSTAS,[1] A. A. KIRATZI,[1] E. E. PAPADIMITRIOU[1] and C. B. PAPAZACHOS[2]

[1]Geophysical Laboratory, Aristotle University of Thessaloniki, GR 540 06 Thessaloniki, Greece
[2]Institute of Earthquake Engineering and Engineering Seismology, Georgikis Sholis, 46 Thessaloniki, Greece

(Received 4 December 1996; revised 5 August 1997; accepted 14 August 1997)

Abstract—Accurate locations of aftershocks, fault plane solutions for the main shock and for a large number of aftershocks as well as geographical distribution of macroseismic intensities led to a reliable estimation of the fault parameters and to a better understanding of the rupture process for the 1995 Kozani–Grevena destructive earthquake. The corresponding fault has a length $L = 30$ km, a width $w = 10$ km, strikes in an ENE direction (N65°E), dips to NNW and the mean displacement on the fault during the generation of this earthquake is about 50 cm. Aseismic preshock slip in an aseismic area of the central part of the fault induced high tectonic stress in the rest of the fault. This stress reached the foreshock barrier's strength near the shallow western boundary of the aseismic area, where the two largest foreshocks occurred, and then the ultimate mainshock barrier's strength near the deep eastern boundary of the aseismic area where the mainshock occurred. From the focus of the mainshock, which was located in the deepest and northernmost part of the fault, the rupture propagated both up-dip and bilaterally and terminated vertically at a depth of about 4 km (blind fault) and horizontally at the eastern and western end of the aftershock zone. The vertical termination of the rupture not at the surface but at some depth is attributed to properties of the uppermost part of the crust or to slipping on minor shallow faults, while the horizontal east and west termination to the intersection of this fault with other faults which strike in a NE direction (geometrical barriers). © 1998 Published by Elsevier Science Ltd. All rights reserved

INTRODUCTION

On Saturday, 13th May 1995, a strong damaging earthquake with magnitude $M_w = 6.5$, occurred in Northwestern Greece (40.13°N–21.67°E). This event attracted the attention of

*Author to whom all correspondence should be addressed: Tel.: 0030 31 998486; Fax: 0030 31 998528.

many scientists since it is the largest instrumentally recorded event in a region which was considered to be of low seismicity (Papazachos and Papazachou, 1989). The earthquake caused extended damage in many villages located within the epicentral area. The two largest cities, Kozani and Grevena, were also considerably affected. Fortunately, no people were killed and only 20 light injuries were reported. This happened because foreshocks with magnitudes $M = 3.8$–4.5 which occurred during the last five minutes before the mainshock led people outside their houses and because, since it was Saturday, several schools which collapsed were empty.

The epicentral area lies in the western margin of the Pelagonian geotectonic zone (Mountrakis, 1986). Neotectonic studies (Pavlides and Mountrakis, 1987; Pavlides and Simeakis, 1988) have shown that the area is dominated by NE–SW striking neotectonic active faults. One of these faults in western Macedonia is the Aliakmon river valley fault that forms the exit of the river to the Aegean sea.

A very high aftershock activity followed this earthquake and a great number of aftershocks were recorded by the Greek seismological network. The data up to the end of August 1995, as well as the available focal mechanisms of the mainshock, were used by Papazachos *et al.* (1995) to define some focal properties of the seismic sequence. According to this paper, the sequence is due to a normal fault which strikes in an ENE–WSW direction and dips to NNW with the mainshock generated in the central, deepest part of the fault under the Vourinos mountain and then the rupture propagated upwards and bilaterally towards the shallow part of the fault.

The day after the main shock, an installation of a portable seismological network around the epicentral area started and was in operation for almost one month. This network, which was installed by the Geophysical Laboratory of the University of Thessaloniki, the Seismological Laboratory of the University of Athens, the Seismological Laboratory of the University of Grenoble and the National Institute of Geophysics of Rome, was in full operation during the time period 19–25th May 1995. At this time forty digital and analog seismographs were deployed. The spacing between the stations was less than 5 km and they covered the rupture zone very well. Several thousands of aftershocks were recorded and Hatzfeld *et al.* (1997) located 622 with a precision better than 1 km. They computed 181 focal mechanisms, which mostly show normal faulting, and observed that the aftershock seismicity is restricted between 5 and 15 km depth and defines a plane dipping North at an angle of about 35°, on which the mainshock probably occurred.

Field observations have been also made by the Laboratory of Geology of the University of Thessaloniki (Mountrakis *et al.*, 1995) with the main goal of identifying surface traces of the seismogenic fault. They identified several ground fissures of normal character with lengths up to 15 km. The most important of these fissures have an ENE strike, dip to NNW, a normal fault slip (1–15 cm) with a small strike-slip component and are located along a line following the villages of Rymnio–Palaeochori–Sarakina.

In the present paper, spatial distribution of accurately determined aftershocks, reliable fault plane solutions of the main shock and aftershocks of the sequence and geographical distribution of high value ($I > VI$) macroseismic intensities are used to define as accurately as possible the orientation, dimensions and slip on the fault which generated the Kozani–Grevena, 15th May 1995 strong earthquake. Some other problems are also discussed, such as the physical process which lead to this seismic excitation, the distribution of the displacements on the fault plane and the probable relation of water loading in the nearby artificial Lake Polifitou with the occurrence of this seismic sequence.

DATA USED

The data concerning the space coordinates of the shocks are travel times of aftershocks recorded by the local network of stations which was operating in the epicentral area during the time period 19–25th May 1995 (Hatzfeld *et al.*, 1997) and travel times of strong shocks (foreshocks, mainshock, aftershocks with $M \geqslant 4.0$) recorded by the regional permanent network of stations in Greece (operated by the Geophysics Laboratory of the University of Thessaloniki and the Geodynamic Institute of the National Observatory of Athens). A 3-D crustal structure model determined for this area (Papazachos *et al.*, 1997) has been used to calculate geographic coordinates of epicenters and focal depth. The 3-D model was used to determine epicenters and focal depths of 665 aftershocks with $M \geqslant 2.3$ which were recorded by the local dense network of stations. The mean error in the determination of the focal coordinates of these aftershocks is equal to $\mathrm{RMS} = 0.14 \pm 0.03$. Most of the differences between the epicenters and the focal depths of the earthquakes located by using the arrivals at the permanent seismological stations in this work, and the epicenters and the focal depths of the same earthquakes located by the local network are less than 5 km. For only a few aftershocks with small magnitudes ($M_L < 4.0$) the differences are larger. The mean difference between the epicenters and the focal depths of the earthquakes with $M_L \geqslant 4.0$ is 2.62 ± 1.97 km and 2.34 ± 1.85 km, respectively. This means that the difference in the location is a consequence of the phase picking and not of the model used. The aftershocks with smaller magnitudes that do not have clear arrivals at the distant stations are not accurately located. For this reason, only the aftershocks with $M_L \geqslant 4.0$ are used in the present study.

Forty-five of these aftershocks, which were accurately located by the local network, were also recorded by the stations of the permanent regional network. By fixing the solutions (origin times, hypocenters) determined by the local network for the 45 shocks, travel time residuals in respect to the 3D model have been calculated for the permanent stations and the average of these residuals for each such station was used to correct the travel times. These corrected travel times of mainly P and some S waves were finally used to locate the main shock and the aftershocks with $M \geqslant 4.0$.

The fault plane solution determined by the GSJ (Geological Survey of Japan) was adopted for the main shock. Fault plane solutions determined by Hatzfeld *et al.* (1997) for 177 aftershocks recorded by the local network of stations are also used in the present study.

Macroseismic intensities of the main shock used in the present study are those published by the Geodynamic Institute of the National Observatory of Athens. These are in the MCS scale which is very similar to MM or MKS scales.

Magnitudes of earthquakes used in the present study are equivalent to moment magnitudes because, although they have been calculated by the use of local data (amplitudes, duration), they were properly corrected (Papazachos *et al.*, 1997) to get values equivalent to moment magnitudes.

SPATIAL DISTRIBUTION OF THE SHOCKS

Figure 1 is a map of the area showing the epicenters of the main shock (star), the two largest foreshocks (triangles), the five largest ($M \geqslant 5.0$) aftershocks (gray circles), the epicenters of 113 aftershocks with $M \geqslant 4.0$ (open circles) and the epicenters of 69 small ($3.6 \leqslant M \leqslant 4.4$) aftershocks (small black circles) which have been located by the dense

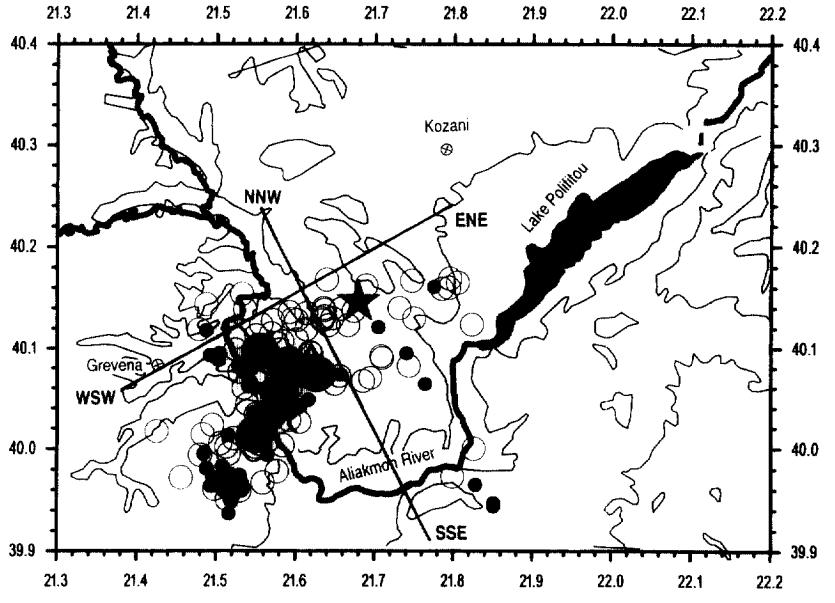

Fig. 1. Epicenters of shocks of the 1995 seismic sequence in the Kozani–Grevena area. Epicenter of the main shock (star), the two largest foreshocks (triangles), the five largest ($M \geq 5.0$) aftershocks (gray circles), the epicenters of 113 aftershocks with $M \geq 4.0$ (open circles) and the epicenters of 69 small ($3.6 \leq M \leq 4.4$) aftershocks (black circles). The smaller aftershocks (black circles) have been located by data of the dense local network of stations, while the other shocks by data of the regional network of permanent stations. Topography contours have been drawn at 300 m intervals.

local network of stations. The main cluster of epicenters has an ENE trend and cover the same area where the most important (I $\geqslant$ VIII) macroseismic effects (Papazachos *et al.*, 1995) and ground fissures were observed after the occurrence of the main shock. It is, however, interesting to note that the largest aftershocks and the two largest foreshocks are located in the western part of the fault zone while the aftershock activity is rather small in the eastern part where the artificial lake Polifitou terminates.

Figure 2 shows a space-time plot of the same data used in Fig. 1. Distance is measured in kilometers along the strike (ENE) of the zone and time in days from the origin time of the main shock. The fault length is defined by the distribution of the accurately located shocks (small black circles in Figs 1 and 2). This length, which presumably is the fault length, is equal to 30 km, and corresponds well to the expected fault length for an earthquake of magnitude $M_w = 6.5$ according to the relation

$$\log L = 0.51M - 1.85 \Rightarrow L = 29\,\text{km} \tag{1}$$

which holds between the fault length and the surface wave magnitude of earthquakes in Greece (Papazachos and Papazachou, 1989).

In order to investigate the vertical distribution of the foci of this sequence data for the most accurately located shocks were used. Such shocks are those recorded by the dense local network of stations and the largest, better located, shocks ($M \geqslant 5.0$) recorded by the regional network.

A cross section normal to the trend of the main cluster of epicenters, that is, in a N65°E

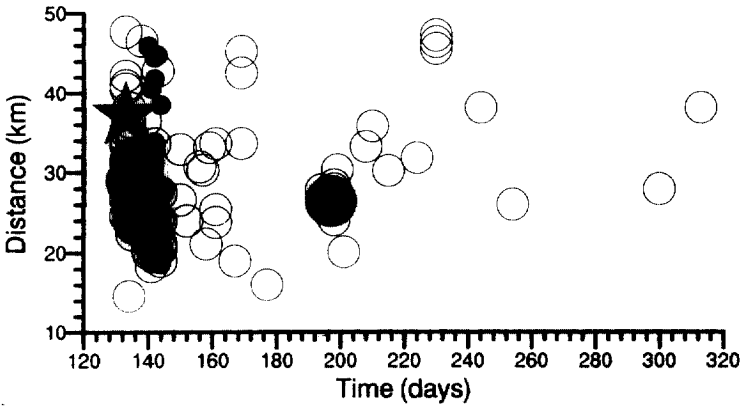

Fig. 2. Space-time plot of the shocks of the 1995 Kozani–Grevena seismic sequence. Data and symbols are the same as in Figure 1. Distance is measured in km along strike of the fault and time in days from the origin time of the mainshock.

direction is shown in Fig. 3 for the shocks located by the local network (small black circles) and the large ($M \geqslant 5.0$) aftershocks located by the regional network (gray circles). In the same figure, the plot for the main shock (star) and for the two largest foreshocks (triangles) are shown. Although a large scatter of the earthquake foci is observed in this vertical cross section, a dipping of the seismic zone in the NNW direction is indicated with the focus of the main shock at the deepest part of the zone. An interesting feature of this plot is that almost all foci are located between 3 km and 13 km depths. The width of the seismic zone, which is presumably the width of the active part of the fault, is about 10 km.

The mean displacement, u (in cm), at the focus of this earthquake can be calculated by the formula:

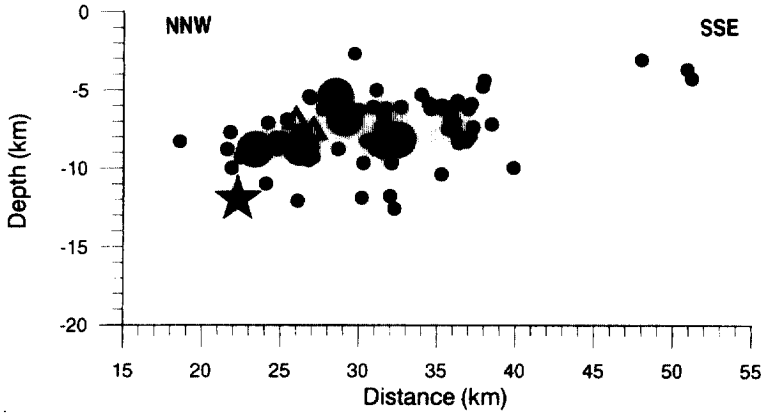

Fig. 3. Cross section normal to the fault strike, (section NNW–SSE in Fig. 1). Small black circles represent the shocks located by the local network and the gray circles represent the shocks with $M \geq 5.0$ located by the regional network.

$$u = \frac{M_0}{\mu/w} \tag{2}$$

where M_0 is the seismic moment, which has been calculated by Harvard and was equal to 7.64×10^{25} dyn cm, μ ($=5 \times 10^{11}$ dyn cm^{-2}) is the shear modulus and L ($=30$ km) and w ($=10$ km) are the dimensions of the fault. Application of this formula gives $u=50$ cm, which is in agreement with the expected displacement for a shallow earthquake with $M=6.5$ according to the formula:

$$\log u = 0.82M - 3.71 \Rightarrow u = 42 \text{ cm} \tag{3}$$

which holds for shallow earthquakes in Greece (Papazachos and Papazachou, 1989).

Figure 4 shows the distribution of the earthquake foci on a vertical plane that cuts the Earth's surface along the strike of the seismic zone (WSW–ENE) which is considered as the strike direction of the fault. The symbols are the same as Fig. 1. It can be deduced from this figure that the fault plane can be separated in the western part, where all of the strong aftershocks ($M \geqslant 5.0$), foreshocks and most of the smaller aftershocks occur, in the central part, of which a considerable area is aseismic, and in the eastern part where the main shock and some not very large aftershocks ($M \leqslant 3.9$) occurred. The seismic activity started by the occurrence of the foreshocks in the western boundary of this aseismic area and the main-shock occurred near the deep eastern boundary of the aseismic area (see Fig. 4). Then, the aftershock activity started in the eastern part of the fault plane (see Table 1) and continued after that mainly in the western part of the plane. It seems therefore, that the central aseismic part of the fault plane, which is under, or very close to the artificial lake Polifitou, played an important role for the initiation of this seismic excitation.

FAULT PLANE SOLUTIONS

Reliable fault plane solutions are available for the main shock, determined by inversion by GSJ (Geological Survey Japan) and Hatzfeld *et al.* (1997), and for 177 aftershocks ($2.7 \leqslant M \leqslant 4.4$) determined by Hatzfeld *et al.* (1997) using first onsets at stations from the

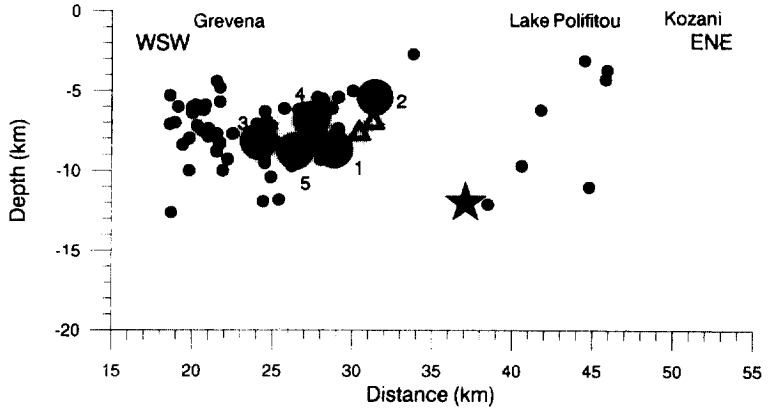

Fig. 4. Vertical section along the fault strike (section WSW–ENE in Fig. 1) of the foci of the most accurately located shocks of the Kozani–Grevena seismic sequence. The numbers next to the large aftershocks denote their sequential occurrence. Symbols are the same as in Figure 1.

Table 1. Source parameters of the earthquakes with $M \geq 4.0$ which were recorded by the regional network during the time period May–November 1995 and have been used in the present study

Date	Or. time	Lat. (N)	Long. (E)	Depth	M	No	RMS
950513	08:43:17.02	40.094	21.619	7.0	4.5	16	1.165
950513	08:47:1.51	40.082	21.611	7.7	4.2	13	0.375
950513	08:47:14.72	40.146	21.679	14.0	6.6	10	0.316
950513	09:01:4.82	40.124	21.823	12.5	4.2	11	0.448
950513	09:47:43.31	40.140	21.731	10.6	4.4	21	0.541
950513	10:11:59.47	40.082	21.743	13.5	4.3	15	0.451
950513	10:33:7.64	40.119	21.613	0.3	4.4	18	0.705
950513	10:58:35.99	40.107	21.583	8.9	4.4	19	0.550
950513	11:43:31.88	40.130	21.646	10.3	4.9	14	0.392
950513	14:16:31.39	40.132	21.636	9.4	4.1	15	0.379
950513	18:06:1.42	40.139	21.657	4.7	4.8	20	0.876
950513	19:00:50.25	40.130	21.750	0.3	4.6	19	1.030
950513	23:53:43.31	40.034	21.550	6.7	4.3	17	0.576
950513	23:56:27.27	40.026	21.580	0.3	4.8	16	0.443
950514	01:02:60.00	40.105	21.576	0.3	4.3	21	0.716
950514	02:38:57.70	40.093	21.566	0.3	4.2	17	0.513
950514	02:47:1.05	40.099	21.579	0.3	4.7	19	0.601
950514	03:02:28.55	40.074	21.556	0.3	4.5	18	0.661
950514	03:09:38.87	40.096	21.618	8.4	4.6	19	0.437
950514	04:29:25.17	40.162	21.689	11.4	4.0	17	0.475
950514	05:14:53.72	40.085	21.583	0.3	4.1	18	0.551
950514	05:59:17.13	40.066	21.551	4.8	4.7	21	0.519
950514	06:27:8.76	40.017	21.425	8.2	4.4	16	0.531
950514	08:35:11.70	40.124	21.556	0.6	4.3	20	0.990
950514	09:45:41.99	40.137	21.673	10.3	4.4	23	0.499
950514	14:46:57.66	40.123	21.666	9.0	4.5	25	0.584
950514	21:31:13.32	40.074	21.637	1.6	4.2	25	0.661
950515	00:24:19.98	40.139	21.536	14.6	4.2	21	0.509
950515	01:20:17.04	40.113	21.550	13.6	4.3	24	0.673
950515	04:13:56.49	40.083	21.591	8.7	5.1	25	0.812
950515	06:42:29.23	40.168	21.639	0.5	4.0	12	0.862
950515	08:17:0.54	40.111	21.525	3.9	4.5	19	1.479
950515	09:01:52.79	40.086	21.566	0.3	4.1	24	0.453
950515	09:19:45.12	40.144	21.487	13.8	4.4	27	0.475
950515	17:05:42.99	40.076	21.556	2.8	4.4	25	0.565
950515	22:47:34.76	40.140	21.635	14.4	4.1	26	0.490
950516	04:37:28.58	40.016	21.554	1.4	4.4	28	0.567
950516	17:57:51.60	40.061	21.594	3.9	4.4	27	0.443
950516	21:54:17.34	40.033	21.557	1.9	4.3	30	0.579
950516	23:00:41.93	40.031	21.572	0.3	4.7	28	0.674
950516	23:57:28.48	40.095	21.619	3.3	4.9	28	0.597
950517	03:54:54.13	40.082	21.615	3.5	4.3	18	0.664
950517	04:14:25.94	40.074	21.626	5.4	5.3	25	0.734
950517	04:48:35.42	40.072	21.595	7.8	4.4	28	0.638
950517	09:45:7.92	40.014	21.549	8.2	5.0	28	1.248
950517	10:07:38.63	40.009	21.543	7.4	4.0	29	0.697
950517	11:25:28.70	40.003	21.584	0.3	4.0	22	0.845
950517	11:28:38.34	40.028	21.592	0.3	4.0	27	0.609
950517	11:36:49.06	40.006	21.563	3.7	4.1	21	0.300
950517	15:38:0.49	40.040	21.569	1.7	4.1	24	0.378

Table 1—*continued*

Date	Or. time	Lat. (N)	Long. (E)	Depth	M	No	RMS
950517	23:51:48.45	40.026	21.605	0.8	4.0	29	0.509
950518	03:49:1.76	40.070	21.627	9.7	4.0	28	0.667
950518	06:22:55.28	40.019	21.550	3.9	4.6	27	0.470
950518	15:26:42.16	40.169	21.795	8.0	4.1	29	0.435
950519	01:03:41.69	40.034	21.572	9.3	4.1	31	0.102
950519	01:30:24.21	40.036	21.575	6.5	4.0	26	0.094
950519	01:33:54.75	40.024	21.563	11.3	4.0	18	0.089
950519	06:48:50.62	40.054	21.580	6.8	5.1	25	0.675
950519	07:36:49.13	40.041	21.586	8.8	4.8	27	0.086
950519	12:29:53.43	40.070	21.694	6.5	4.0	25	0.371
950519	13:07:48.74	40.002	21.549	9.4	4.1	15	0.662
950520	20:09:30.81	39.951	21.514	7.2	4.3	38	0.105
950520	20:11:53.03	39.961	21.517	5.8	4.1	34	0.096
950520	21:06:24.07	39.966	21.526	9.1	4.5	27	0.101
950520	21:19:34.99	40.070	21.596	5.6	4.1	46	0.087
950520	22:24:59.52	39.959	21.530	4.5	4.0	45	0.094
950521	04:04:21.83	39.994	21.480	12.7	4.4	36	0.129
950521	20:38:26.80	40.119	21.478	9.5	4.2	51	0.091
950522	20:21:34.29	40.081	21.537	9.3	4.4	47	0.100
950522	21:10:33.22	39.971	21.513	7.9	4.1	46	0.101
950522	22:30:41.13	40.072	21.655	2.8	4.2	27	0.093
950523	04:37:39.93	40.076	21.529	9.9	4.2	47	0.096
950523	05:51:58.87	40.167	21.747	12.8	4.1	39	0.099
950523	20:09:53.96	40.010	21.522	3.7	4.3	31	0.447
950523	20:59:51.05	40.005	21.554	3.1	4.2	24	0.508
950524	05:22:43.51	40.060	21.534	10.7	4.0	49	0.090
950524	06:24:8.37	39.961	21.498	8.5	4.4	52	0.102
950524	07:00:3.05	40.002	21.513	4.6	4.3	30	0.519
950524	14:45:22.93	40.005	21.505	5.4	4.0	85	0.459
950524	17:34:26.71	40.066	21.576	6.6	4.1	41	0.100
950530	12:06:43.25	40.064	21.649	4.0	4.4	32	1.051
950530	14:30:2.85	40.003	21.584	6.2	4.4	27	0.488
950602	07:47:15.79	40.044	21.539	3.4	4.0	27	0.380
950606	04:35:59.45	40.128	21.601	6.5	4.8	28	0.420
950607	08:37:35.14	40.129	21.596	3.4	4.3	26	0.709
950608	02:13:48.18	39.995	21.516	13.6	4.6	27	0.549
950609	15:20:49.07	40.128	21.633	2.5	4.3	20	0.419
950611	17:20:11.31	40.138	21.636	1.5	4.0	26	0.328
950611	18:51:47.85	39.967	21.559	4.5	4.8	25	0.427
950611	20:38:22.72	39.978	21.577	5.0	4.0	24	0.318
950617	06:14:53.46	40.014	21.483	4.6	4.0	23	0.493
950619	03:53:59.55	40.000	21.826	4.3	4.4	20	0.378
950619	04:41:32.05	40.123	21.641	3.4	4.1	22	0.556
950619	15:00:21.27	39.973	21.799	6.0	4.2	20	0.348
950627	06:33:54.50	39.972	21.456	10.5	4.0	D10	0.294
950714	21:19:38.93	40.039	21.589	0.3	4.0	21	0.594
950717	23:18:15.44	40.097	21.555	8.8	5.5	24	0.609
950718	03:09:7.66	40.099	21.524	7.7	4.3	21	0.713
950718	05:05:33.47	40.115	21.569	0.3	4.3	24	0.506
950718	07:42:54.69	40.128	21.571	7.6	4.7	27	1.034
950719	18:23:15.10	40.109	21.601	12.3	4.7	25	0.774

Table 1—*continued*

Date	Or. time	Lat. (N)	Long. (E)	Depth	M	No	RMS
950721	13:27:46.77	40.023	21.495	18.5	4.1	23	0.623
950728	22:43:30.52	40.130	21.633	7.0	4.3	27	0.820
950730	09:28:11.12	40.067	21.685	10.4	4.0	25	0.683
950805	18:14:43.06	40.136	21.592	4.5	4.0	24	0.542
950814	17:57:4.36	40.135	21.613	3.5	4.2	27	0.492
950820	18:53:11.75	40.159	21.785	11.2	4.1	18	0.416
950820	19:21:24.36	40.160	21.794	11.4	4.2	30	0.401
950820	19:27:52.32	40.165	21.805	9.3	4.2	25	0.512
950904	04:09:24.88	40.090	21.709	6.7	4.1	27	0.641
950914	01:26:39.90	40.154	21.532	3.9	4.2	28	0.721
951030	01:53:12.38	40.049	21.588	8.5	4.0	26	0.740
951113	13:40:33.96	40.092	21.708	5.9	4.0	24	0.672

dense local network. The fault plane solutions of the aftershocks were used to determine the 'representative focal mechanism tensor, F' by a procedure suggested by Papazachos and Kiratzi (1992).

Table 2 shows the fault plane solution for the mainshock and the representative fault plane solution obtained from the aftershocks. Plane A is considered to be the fault plane on the basis of the spatial distribution of the aftershock foci (Fig. 1), macroseismic information and surface fault traces (Papazachos *et al.*, 1995; Mountrakis *et al.*, 1995). The similarity of the two solutions listed in Table 2, which were determined by different data and different methodology, is striking and suggests that the focal mechanism of the mainshock is also expressed in the 'mean focal mechanism' of its aftershocks.

A careful examination by the use of the "RAKE" software (Louvari and Kiratzi, 1997) of the individual mechanisms of the aftershocks revealed that although all mechanisms have a dip-slip normal component, a number of them have a considerable strike-slip component. This scattering can be attributed to uncertainties in the determination of the fault plane solutions or a real spatial variation. To examine these possibilities, we defined seven clusters of aftershocks after a careful examination of all the mechanisms, and determined the representative focal mechanisms for each one of these clusters. Figure 5 shows the representative focal mechanisms of these clusters, as well as the mechanism of the mainshock and the major surface breaks of the fault. The parameters of the representative focal mechanism for each cluster are listed in Table 3. The information given in this table indicates that the fault plane solutions of the central part of the rupture zone (clusters 1 to

Table 2. The fault plane solution of the mainshock (MS) and the 'representative fault plane solution' of the 177 aftershocks (AF)

	Nodal plane 1			Nodal plane 2			P-axis		T-axis		Eigenvalues		
	strike	dip	rake	strike	dip	rake	Az	plunge	Az	plunge	λ_1	λ_2	λ_3
MS	240	45	−101	75	47	−79	60	82	157	1			
AF	238	48	−106	81	44	−73	78	78	339	2	0.77	−0.07	−0.69

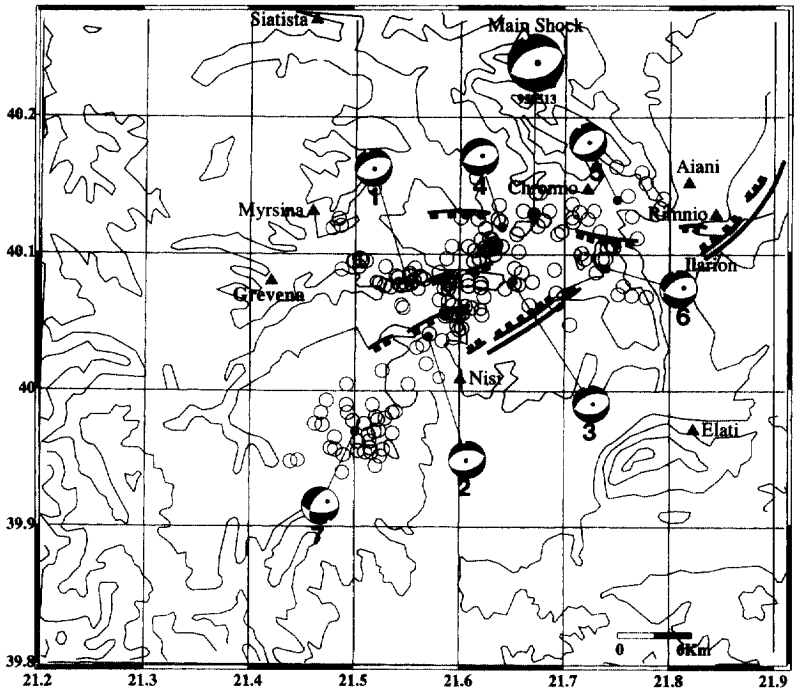

Fig. 5. Fault plane solution of the mainshock of the Kozani–Grevena sequence and the representative fault plane solutions of the seven clusters (1 to 7) of aftershocks (shown with black circles). Ground fissures (hatched lines) and neotectonic faults (thick lines) are those observed by Pavlides *et al.*, 1995.

Table 3. The parameters of the seven representative fault plane solutions shown in Figure 5

No.	Nodal plane 1			Nodal plane 2			P-axis		T-axis		Eigenvalues		
	strike	dip	rake	strike	dip	rake	Az	plunge	Az	plunge	λ_1	λ_2	λ_3
1	247	52	−92	71	38	−87	145	82	339	7	0.80	−0.15	−0.66
2	265	46	−80	71	44	−100	249	83	348	1	0.82	−0.04	−0.78
3	247	49	−100	82	42	−79	98	82	344	3	0.82	−0.05	−0.77
4	242	44	−107	85	48	−74	64	78	164	2	0.72	−0.02	−0.71
5	235	49	−95	63	41	−84	107	84	329	4	0.84	0.06	−0.90
6	235	50	−122	99	50	−58	77	66	347	0	0.69	0.05	−0.74
7	210	56	−138	94	56	−42	62	52	152	0	0.80	−0.01	−0.80

5) are very similar. For this reason a representative fault plane solution for all events of these five clusters has been determined (Table 4). It indicates an almost pure normal faulting for the central part.

On the contrary, the fault plane solutions close to the northeastern end (cluster 6) and to the southwestern end (cluster 7) indicate normal faulting with considerable strike-slip component (rake = -58° or -122° for cluster 6 and -42° or -138° for cluster 7).

One explanation is that in the central part of the aftershock zone, the faulting is new and

Table 4. Representative fault plane solution for the central part (clusters 1 to 5) of the rupture zone (Fig. 5)

Nodal plane 1			Nodal plane 2			P-axis		T-axis		Eigenvalues		
strike	dip	rake	strike	dip	rake	Az	plunge	Az	plunge	λ_1	λ_2	λ_3
246	48	−97	76	42	−82	103	84	341	3	0.78	−0.06	−0.72

is a result of the action of the present day regional horizontal tension in a NNW direction (~N20°W) (Papazachos and Kiratzi, 1996), and for this reason, faulting occurs in a ENE direction (~N70°E, see Table 4). In the eastern end of the rupture zone, a geometric barrier exists, since it is the area where the Servia normal fault starts (Mountrakis *et al.*, 1995). This Servia fault has a NE strike and dips to the NW (see Fig. 5). Thus, the strike of this fault forms a smaller than 90° angle with the present regional tension. Therefore, earthquakes at the Servia zone under the present regional stress field will exhibit normal faulting with a considerable strike-slip (dextral) component. The same reasoning can be applied to the southwestern end of the rupture zone because the distribution of the aftershock epicenters there (cluster 7) indicates a change of the fault strike to a more NNE–SSW direction.

Figure 6 schematically shows the interpretation of the variation of the fault plane solutions of the aftershocks from pure normal faulting in the main central part of the fault to normal with a dextral strike-slip component near the ends of the zone. The active regional tension is horizontal and has a NNW direction causing pure normal in the central part of the rupture zone that has a ENE strike, while at the two ends where the fault changes its

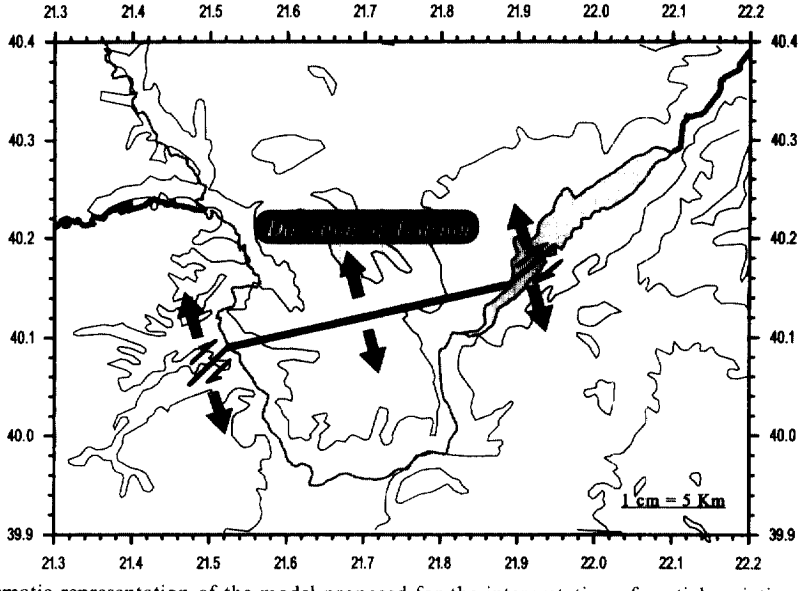

Fig. 6. Schematic representation of the model proposed for the interpretation of spatial variation of the focal mechanisms of the aftershocks. The active regional tension caused normal faulting in the central main part of the aftershock zone and normal with a strike-slip component faulting at the two ends due to the intersection of the fault with other faults striking NE.

strike to a NE direction, the same tension causes normal faulting with a dextral strike-slip component.

MACROSEISMIC FIELD

Macroseismic information near the epicentral area has been used to define the rupture zones of strong earthquakes because such zones are the areas of high macroseismic intensity. Evidence has been presented that the isoseismal of intensity I = VIII (in the MM scale) defines the rupture zone and the direction of the major axis of the high intensity isoseismals coincides with the fault strike.

Papazachos (1992) developed a method to define the synthetic isoseismals by the use of macroseismic intensities of shallow earthquakes taking also into consideration anisotropic radiation at the seismic source, geometrical spreading and anelastic attenuation. This method, among others, also gives the macroseismic magnitude M ($\sim M_w$), the ellipticity, e, and the azimuth, z of the maximum axes of the isoseismals and has been applied to the macroseismic intensities of I $\geqslant$ VI by which the mainshock of the Kozani–Grevena seismic sequence was felt at 45 places in northern Greece. These macroseismic data (intensities and corresponding places) are published in the July 1995 bulletin of the Geodynamic Institute of the National Observatory of Athens.

Figure 7 shows the synthetic isoseismals of I = IX, VIII, VII and VI as well as the distribution of the macroseismic intensities which were used to define them. The macroseismic magnitude, the azimuth of the major axes of the isoseismals and the length of the isoseismal of intensity VIII are equal to $M = 6.4$, $z = 65^\circ$ and $L = 35$ km, respectively. All these macroseismic parameters are in good agreement with the corresponding parameters defined by other methods, since the instrumentally determined magnitude is $M_w = 6.5$ (Harvard determination), the strike of the fault plane is 60° (see Table 2) and the fault length defined by the aftershock zone is 30 km.

DISCUSSION

The lack of considerable aftershock activity in an area of the central part of the seismic fault and in the uppermost crustal layers (depths less than about 3 km, see Fig. 4) requires some further discussion. A consequence of the barrier model (Aki, 1979) is that strong aftershocks occur in those parts of fault plane where strong barriers exist and no *soon-to-break* barriers exist in those areas of the fault plane where the aftershock activity is reduced. With this reasoning, either pre-seismic aseismic slip is possible in areas of reduced aftershock activity, or the stress is released during the occurrence of the mainshock. Such areas of reduced aftershock activity have been observed in the central parts of the fault planes in all cases of recent, and better studied, strong shallow earthquakes in Greece. These areas have been considered as regions where preseismic slip, which induced high tectonic stress in the fault, occurs (Rocca *et al.*, 1985; Karakaisis *et al.*, 1985; Papazachos *et al.*, 1988).

Pre-seismic aseismic slip in the shallow central area of the fault induced additional tectonic stress, causing the breakage of barriers and the generation of foreshocks (with magnitude up to 4.5) close to the western boundary of the area of aseismic slip (Fig. 4). The aseismic deformation continued and was probably accelerated after the generation of foreshocks. In this way, it induced high tectonic stress which in few minutes reached the mainshock's barrier ultimate strength and resulted in the generation of the mainshock close

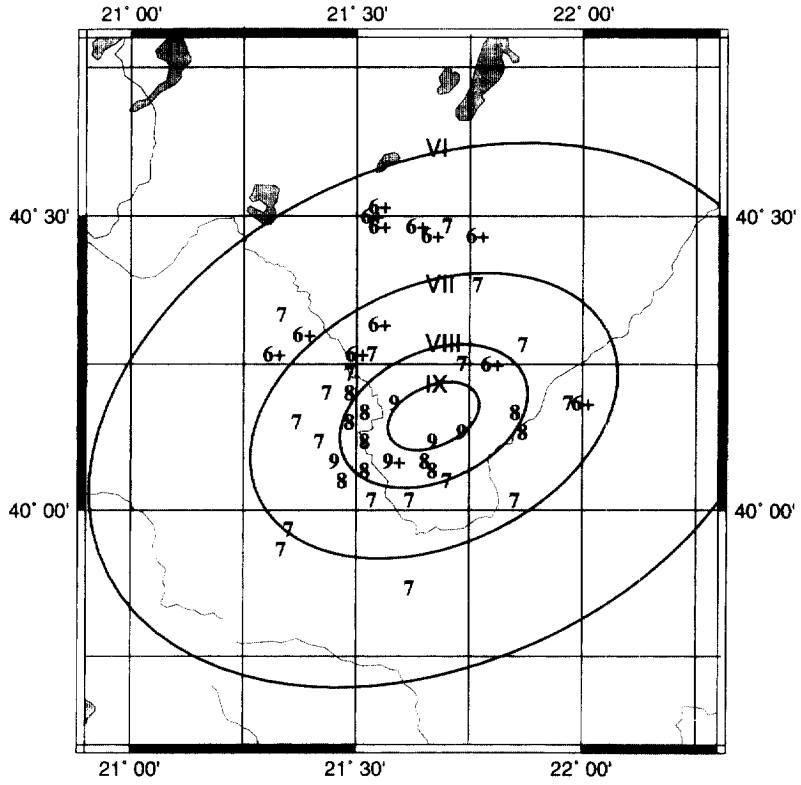

Fig. 7. Geographic distribution of macroseismic intensities (I ≥ VI) and synthetic isoseismals for the 1995 Kozani–Grevena earthquake.

to the deepest and eastern boundary of the aseismic deforming area. The generation of the mainshock caused a redistribution of stresses and their concentration, mainly at barriers of the western part of the fault where aftershocks occurred. Also, the fact that the area of aseismic slip is under, or very close to, the artificial lake Polifitou indicates that the water loading in this place facilitated this aseismic deformation.

The displacement measured at the surface fault fissures (Mountrakis *et al.*, 1995) is small (~ 10 cm) in relation to the mean slip calculated for the whole fault (~ 50 cm). The vertical distribution of the aftershock foci (Fig. 3 and 4) indicates that most of the slip occurred at depths between 4 km and 14 km where all the large earthquakes of the sequence and the majority of the small earthquakes occurred. Therefore, the fault can be considered as a blind normal fault, in the sense that rupture initiated at the depth of the focus of the mainshock (~ 12 km), propagated up-dip and bilaterally and terminated at a depth of about 4 km. This kind of rupture has been suggested for the Loma Prieta 1989 earthquake and the low stress in the uppermost crust was attributed to

(a) genuine changes in the rock material between the upper and lower crust,
(b) to stress relief by slip on minor faults in the upper crust or,
(c) to stress relief in the upper crust in a previous earthquake (Wallace and Wallace, 1993).

Since no strong earthquake occurred in the Kozani–Grevena area for about three hundred years before the 1995 event the third explanation cannot be applied in the present case.

Therefore, the vertical termination of the rupture at some depth can be attributed to properties of the uppermost part of the crust, while the horizontal termination of the fault in the eastern as well as in the western part of the aftershock zone is due to its intersection with preexisting faults of a different orientation.

Acknowledgements—This work was partially supported by the EC Environment Research Program (ENV4-CT96-0277), Climatology and Natural Hazards.

REFERENCES

Aki, K. (1979) Characterization of bearriers on an earthquake fault. *J. Geophys. Res.* **84,** 6140–6148.

Hatzfeld, D., Karakostas, V., Ziazia, M., Selvaggi, G., Leborgne, S., Berge, C., Guiguet, R., Paul, A., Voidomatis, Ph., Diagourtas, D., Kassaras, I., Koutsikos, I., Makropoulos, K., Azzara, R., Di Bona, M., Bacchechi, S., Bernard, P. and Papaioannou, Ch. (1997) The Kozani–Grevena (Greece) earthquake of 13th May 1995, revisited from a detailed seismological study. *Bull. Seism. Soc. Am.* **87,** 463–473.

Karakaisis, G. F., Karacostas, B. G., Papadimitriou, E. E., Scordilis, E. M. and Papazachos, B. C. (1985) Seismic sequences in Greece interpreted in terms of the barrier model. *Nature* **315,** 212–214.

Louvari, E. and Kiratzi, A. (1997). "Rake": A window's program to plot earthquake focal mechanisms and stress orientation. *Computers and Geosciences* **23,** 851–857.

Mountrakis, D. (1986) The Pelagonian zone in Greece: a Polyphase deformed fragment of the cimmerian continent and its role in the geotectonic evolution of east mediterranean. *J. of Geology* **94,** 335–347.

Mountrakis, D., Pavlides, S., Zouros, N., Chatzipetros, A. and Kostopoulos, D. (1995). The 13th May 1995, Western Macedonia (Greece) earthquake. Preliminary results on the seismic fault geometry and kinematics. In *XV Congress of the Carpatho–Balkan Geological Association*, September 17–20, 1995, Athens, Greece, 11 pp.

Papazachos, B. C., Kiratzi, A. A., Karacostas, B. G., Panagiotopoulos, D. G., Scordilis, E. M. and Mountrakis, D. M. (1988) Surface fault traces, fault plane solution and spatial distribution of the aftershocks of the September 13, 1986 earthquake of Kalamata (Southern Greece). *Pure and Applied Geophysics* **126**(1), 55–68.

Papazachos, B. C. and Papazachou, C. B. (1989) *The earthquakes of Greece*, 356 pp. Ziti Publications, Thessaloniki, Greece.

Papazachos, B. C., Panagiotopoulos, D. G., Scordilis, E. M., Karakaisis, G. F., Papaioannou, Ch. A., Karakostas, B. G., Papadimitriou, E. E., Kiratzi, A. A., Hatzidimitriou, P. M., Leventakis, G. N., Voidomatis, Ph.S., Peftitselis, K. J. and Tsapanos, T. M. (1995). Focal properties of the 13th May 1995 large ($M_s = 6.6$) Earthquake in the Kozani area (North Greece). In *XV Congress of the Carpatho–Balkan Geological Association*, September 17–20, 1995, Athens, Greece, 96–106.

Papazachos, B. C., Kiratzi, A. A. and Karacostas, B. G. (1997) Towards a homogeneous moment-magnitude determination for earthquakes in Greece and the surrounding area. *Bull. Seism. Soc. Am.* **87,** 474–483.

Papazachos, C. B. (1992) Anisotropic radiation modeling of macroseismic intensities for estimation of the attenuation structure of the upper crust in Greece. *Pure and Applied Geophysics* **138,** 445–469.

Papazachos, C. B. and Kiratzi, A. A. (1992) A formulation for reliable estimation of active crustal deformation and its application to central Greece. *Geophys. J. Int.* **111,** 424–432.

Papazachos, C. B. and Kiratzi, A. A. (1996) A detailed study of the active crustal deformation in the Aegean and surrounding area. *Tectonophysics* **253,** 129–153.

Papazachos, C. B., Karakostas, B. G. and Scordilis, E. M. (1997) Crustal and upper mantle structure of the Kozani–Grevena and surrounding area obtained by non-linear inversion of P and S travel times. *J. Geodyn.* **26,** 353–365.

Pavlides, S. and Mountrakis, D. (1987) Extensional tectonics of Northwestern Macedonia, Greece, since the late Miocene. *J. Struct. Geol.* **9,** 385–392.

Pavlides, S. and Simeakis, K. (1988) Neotectonic and active tectonics in low seismicity areas of Greece: Vegoritis (NW Macedonia) and Melos Isl. complex (Cyclades)—Comparison. *Ann. Geol. Pays Hellenique* **33,** 161–176.

Pavlides, S. B., Zouros, N. C., Chatzipetros, A. A., Kostopoulos, D. S. and Mountrakis, D. M. (1995) The 13th May 1995 Western Macedonia, Greece (Kozani Grevena Earthquake; preliminary results. *Terra Nova* **7,** 544–549.

Rocca, A., Karakaisis, G., Karacostas, B., Kiratzi, A., Scordilis, E. and Papazachos, B. (1985) Further evidence on the strike-slip faulting of the Northern Aegean trough based on properties of the August–November 1983 sequence. *Boll. Geof. Teor. Appl.* **27**(106), 101–109.

Wallace, M. H. and Wallace, T. C. (1993) The Paradox of Loma Prieta Earthquake: Why did rupture terminate at depth? *J. Geophys. Res.* **98,** 19859–19867.